Supporting Information

Enhanced Gas Barrier Property of Polymer Substrates for Flexible OLED by Adjusting Backbone Rigidity and Incorporating 2D nanosheets

Zhenghui Yang[a,b], Haiquan Guo[a,*], Chuanqing Kang[a,b] and Lianxun Gao[a]

[a] *State Key Laboratory of Polymer Physics and Chemistry, Changchun Institute of Applied Chemistry, Chinese Academy of Sciences, Changchun 130022, China.*

E-mail: hqguo@ciac.ac.cn

[b] *University of Science and Technology of China, Hefei 230026, China.*

1. *Diffusivity and solubility of oxygen for pure PI films.*

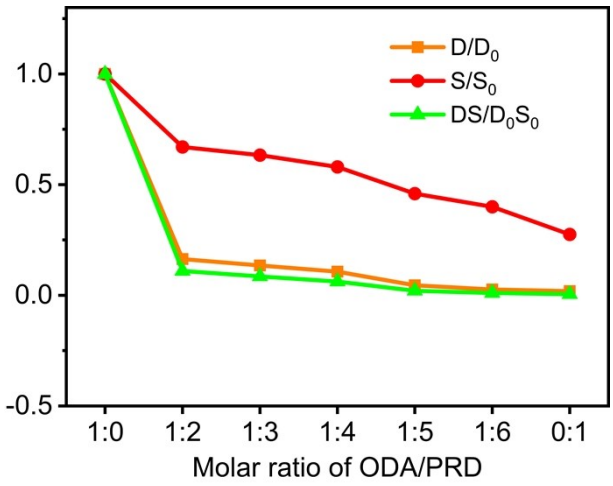

Figure S1 The diffusivity and solubility of oxygen (O_2) for pure PI films.

It was reported by Lim *et al* [1] that gas permeability (P) was correlated with diffusivity (D) and solubility (S) which could be expressed as follows:

$$P = J_s d = SD$$

Where J_s and d represented the gas molar flux at a certain time at steady state and the film thickness, respectively. Herein, the effect of diffusivity and solubility on the oxygen permeability of pure PI films was examined. It should be noted that D_0 and S_0 referred the diffusivity and solubility of PMDA/ODA. As shown in Figure S1, the value of D/D_0 and S/S_0 exhibited a drastic reduction with an increase of PRD content, suggesting the dense packing of rigid-rod molecular chains contributed to the reduction of both diffusivity and solubility, resulting in great oxygen barrier performance. Additionally, as the PRD content increased, the decline of diffusivity was much more prominent than that of solubility for PI films, indicating the former performed a dominant role in the reduction of oxygen permeability.

2. The crystallinity (X_c) of pure PI films

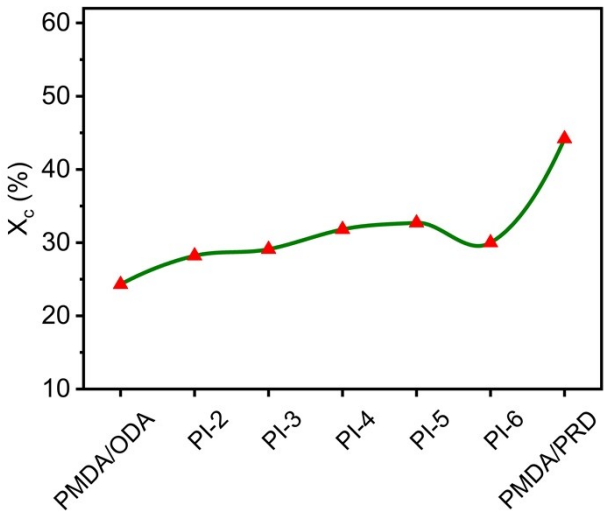

Figure S2 The crystallinity (X_c) of pure PI films.

The crystallinity (X_c) was calculated as follows:[2]

$$X_c = \frac{A_c}{A_c + A_a} \times 100\% \quad (2)$$

Where A_c and A_a were the crystallization peak area and the amorphous peak area, respectively. As depicted in Figure S2, with the incorporation of PRD, the crystallinity (X_c) was obviously increased from 24.3% to 44.2%, which conformed well to the reduction of gas permeability.

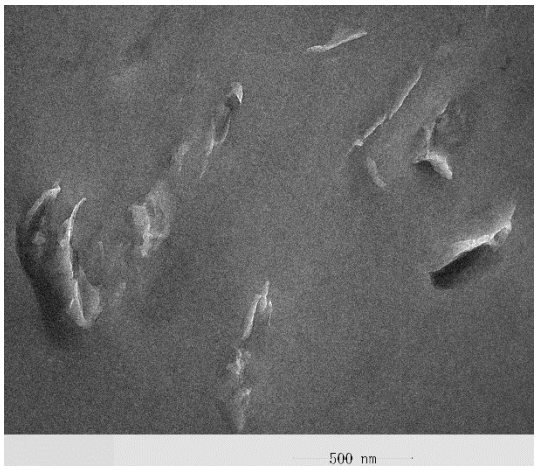

Figure S3 TEM image of PI nanocomposite films at a loading of 3.0% OLDH (PIL-3.0).

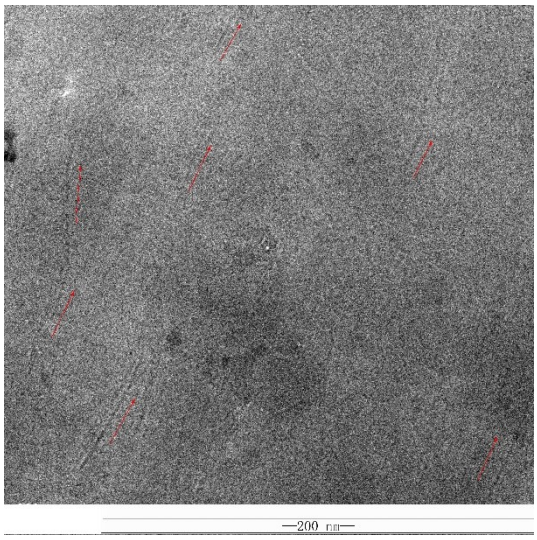

Figure S4 TEM image of PI nanocomposite films at a loading of 1.0% GO (PIG-1.0).

Table S1 Oxygen permeability $P(O_2)$ of various polymer naonocomposite films.

Sample	Filler Type	Filler Content	$P(O_2)$ (cm^3 mm m^{-2} day^{-1} atm^{-1})	Percentage of $P(O_2)$ Reduction	References
PET/LDHs-m5	LDH	5%	2.0	48.7%	Gao *et al* [3]
LLDPE/MMT93 A	MMT	5%	109.08	57.9%	Kalendova *et al* [4]
PET/h-BN	h-BN	3%	1.48	70%	Xie *et al* [5]
PVC/DOP+MMT30B	MMT	10%	61.43	42.3%	Kalendova *et al* [4]
LDH@PDA/PCL	LDH	7%	~60	46.0%	Mao *et al* [6]
PI/MMT	MMT	3%	10.57	69.2%	Huang *et al* [7]
PDMS/GO	GO	8%	236.39	71.7%	Park *et al* [8]
PLA/GOQD0.05	GOQD	0.05%	~14	45.7%	Xu *et al* [9]
PHBH/SiO_2	SiO_2	2.5%	6.58	46.7%	Qiu *et al* [10]
PI/OLDH (PIL)	OLDH	3%	0.345	78.1%	our work
PI/GO (PIG)	GO	0.3%	0.228	85.5%	our work

References

1. Lim, J.; Yeo, H.; Goh, M.; Ku, B.-C.; Kim, S. G.; Lee, H. S.; Park, B.; You, N.-H., Grafting of Polyimide onto Chemically-Functionalized Graphene Nanosheets for Mechanically-Strong Barrier Membranes. *Chemistry of Materials* **2015,** *27* (6), 2040-2047.
2. Liu, J.-J.; Tan, J.-H.; Zeng, Y.; Liu, Y.-W.; Zeng, K.-J.; Liu, Y.-J.; Wu, R.-M.; Chen, H., Synthesis and characterization of high-barrier polyimide containing rigid planar moieties and amide groups. *Polymer Testing* **2017,** *61*, 83-92.
3. Gao, M.; Jiao, Q.; Cui, W.; Feng, C.; Zhao, Y.; Xiang, A.; Mu, X.; Ma, L., Preparation of PET/LDH composite materials and their mechanical properties and permeability for O2. *Polymer Engineering & Science* **2019,** *59* (s2), E366-E371.
4. Kalendova, A.; Merinska, D.; Gerard, J. F.; Slouf, M., Polymer/clay nanocomposites and their gas

barrier properties. *Polymer Composites* **2013,** *34* (9), 1418-1424.

5. Xie, S.; Istrate, O. M.; May, P.; Barwich, S.; Bell, A. P.; Khan, U.; Coleman, J. N., Boron nitride nanosheets as barrier enhancing fillers in melt processed composites. *Nanoscale* **2015,** *7* (10), 4443-50.

6. Mao, L.; Liu, Y.; Wu, H.; Chen, J.; Yao, J., Poly(ε-caprolactone) filled with polydopamine-coated high aspect ratio layered double hydroxide: Simultaneous enhancement of mechanical and barrier properties. *Applied Clay Science* **2017,** *150*, 202-209.

7. Huang, C.-C.; Jang, G.-W.; Chang, K.-C.; Hung, W.-I.; Yeh, J.-M., High-performance polyimide-clay nanocomposite materials based on a dual intercalating agent system. *Polymer International* **2008,** *57* (4), 605-611.

8. Park, J.; Ha, H.; Yoon, H. W.; Noh, J.; Park, H. B.; Paul, D. R.; Ellison, C. J.; Freeman, B. D., Gas sorption and diffusion in poly(dimethylsiloxane) (PDMS)/graphene oxide (GO) nanocomposite membranes. *Polymer* **2021,** *212*.

9. Xu, H.; Adolfsson, K. H.; Xie, L.; Hassanzadeh, S.; Pettersson, T.; Hakkarainen, M., Zero-Dimensional and Highly Oxygenated Graphene Oxide for Multifunctional Poly(lactic acid) Bionanocomposites. *Acs Sustainable Chemistry & Engineering* **2016,** *4* (10), 5618-5631.

10. Qiu, Y.; Fu, J.; Sun, B.; Ma, X., Sustainable nanocomposite films based on SiO2 and biodegradable poly(3-hydroxybutyrate-co-3-hydroxyhexanoate) (PHBH) for food packaging. *E-Polymers* **2021,** *21* (1), 72-81.